Presenilin-1 affects trafficking and processing of βAPP and is targeted in a complex with nicastrin to the plasma membrane

Christoph Kaether,[1] Sven Lammich,[1] Dieter Edbauer,[1] Michaela Ertl,[1] Jens Rietdorf,[2] Anja Capell,[1] Harald Steiner,[1] and Christian Haass[1]

[1]Adolf-Butenandt-Institute, Department of Biochemistry, Laboratory for Alzheimer's and Parkinson's Disease Research, Ludwig-Maximilians-University, 80336 Munich, Germany
[2]Advanced Light Microscopy Facility, European Molecular Biology Laboratories, 69012 Heidelberg, Germany

Amyloid β-peptide (Aβ) is generated by the consecutive cleavages of β- and γ-secretase. The intramembraneous γ-secretase cleavage critically depends on the activity of presenilins (PS1 and PS2). Although there is evidence that PSs are aspartyl proteases with γ-secretase activity, it remains controversial whether their subcellular localization overlaps with the cellular sites of Aβ production. We now demonstrate that biologically active GFP-tagged PS1 as well as endogenous PS1 are targeted to the plasma membrane (PM) of living cells. On the way to the PM, PS1 binds to nicastrin (Nct), an essential component of the γ-secretase complex. This complex is targeted through the secretory pathway where PS1-bound Nct becomes endoglycosidase H resistant. Moreover, surface-biotinylated Nct can be coimmunoprecipitated with PS1 antibodies, demonstrating that this complex is located to cellular sites with γ-secretase activity. Inactivating PS1 or PS2 function by mutagenesis of one of the critical aspartate residues or by γ-secretase inhibitors results in delayed reinternalization of the β-amyloid precursor protein and its accumulation at the cell surface. Our data suggest that PS is targeted as a biologically active complex with Nct through the secretory pathway to the cell surface and suggest a dual function of PS in γ-secretase processing and in trafficking.

Introduction

The two presenilins (PSs),* PS1 and PS2, are key factors in the pathogenesis of Alzheimer's disease (for review see Esler and Wolfe, 2001). Familial Alzheimer's disease (FAD)–associated PS mutations drastically lower the age of onset of the disease. Currently, ~100 mutations (see http://molgen-www.uia.ac.be/ADMutations) have been identified, which apparently all cause the increased production of the highly amyloidogenic 42–amino acid amyloid β-peptide (Aβ42) (Selkoe, 1999).

Amyloid β-peptide (Aβ) is generated from the β-amyloid precursor protein (βAPP) by proteolytic processing mediated by two distinct secretase activities (Esler and Wolfe, 2001). β-secretase (β-site APP cleaving enzyme [BACE]) mediates the NH$_2$-terminal cleavage (Vassar and Citron, 2000) and produces a membrane-bound COOH-terminal fragment of βAPP (βAPP CTF). BACE has an acidic pH optimum and is preferentially active within early endosomes (for review see Vassar and Citron, 2000). Consistent with the acidic pH optimum of BACE, reinternalization of βAPP from the cell surface is required for Aβ generation (Perez et al., 1999). The BACE-generated βAPP CTF can be transported back to the cell surface (Yamazaki et al., 1996), and at or close to the cell surface, the final γ-secretase cleavage takes place, which results in the liberation of Aβ into biological fluids (for review see Selkoe, 1999).

Although β-secretase has been identified (Vassar and Citron, 2000), the nature of γ-secretase is still unknown. Clearly, PSs are required for the intramembraneous γ-secretase cleavage. Gene deletion of PS1 and PS2 fully inhibits γ-secretase activity

and results in the accumulation of the immediate precursors for γ-secretase activity, the βAPP CTF, as well as in a complete loss of Aβ production (Herreman et al., 2000; Zhang et al., 2000). PS inactivation by the mutagenesis of critical aspartates within TM6 and TM7 of PS1 (Wolfe et al., 1999b) and PS2 (Steiner et al., 1999a; Kimberly et al., 2000) also blocks γ-secretase activity. In addition, the critical aspartate in transmembrane domain 7 is located within a conserved domain also found in numerous bacterial aspartyl proteases of the type 4 prepilin peptidase family (Steiner et al., 2000). Therefore, it is tempting to speculate that PSs are aspartyl proteases with γ-secretase activity (Wolfe et al., 1999a). This is also consistent with the finding that inactivation of PSs blocks the intramembraneous cleavage of its other known substrates, Notch 1–4 (De Strooper et al., 1999; Saxena et al., 2001), ErbB4 (Ni et al., 2001), E-cadherin (Marambaud et al., 2002), and LDL receptor–related protein (May et al., 2002). Although this is the most parsimonious conclusion from the above described results, PSs are probably not active by themselves but require the formation of a proteolytically active high molecular weight complex (Capell et al., 1998; Li et al., 2000a). Moreover, the subcellular localization of PSs may not overlap with cellular compartments thought to be involved in Aβ production, i.e., where γ-secretase activity resides (Annaert et al., 1999; Cupers et al., 2001). This phenomenon, now known as the "spatial paradox" (Checler, 2001; Cupers et al., 2001), describes the findings that PSs are predominantly located within early compartments such as the ER and the intermediate compartment (Annaert et al., 1999; Cupers et al., 2001). Careful cellular analysis of PS1 distribution in cultured neurons indeed revealed very little, if any, PS1 beyond these early compartments (Annaert et al., 1999; Cupers et al., 2001). Based on these findings, it was concluded that PSs may not be identical to γ-secretase (Annaert et al., 1999; Cupers et al., 2001), because this protease is thought to be active at or close to the cell surface (Haass et al., 1993). However, a number of studies have found PSs to be localized in post-Golgi compartments (Takashima et al., 1996; Efthimiopoulos et al., 1998; Georgakopoulos et al., 1999; Ray et al., 1999; Schwarzman et al., 1999; Lah and Levey, 2000; Singh et al., 2001).

Recently, nicastrin (Nct) was shown to be a component of the PS complex that is essential for γ-secretase activity (Yu et al., 2000; Chung and Struhl, 2001; Levitan et al., 2001; Edbauer et al., 2002; Hu et al., 2002; Lopez-Schier and Johnston, 2002). Nct is a type I transmembrane protein containing multiple glycosylation sites. In mammalian cells, it is present in an immature, endoglycosidase H (endoH)–sensitive N-glycosylated form, and a mature, endoH-resistant N-glycosylated form (Edbauer et al., 2002; Leem et al., 2002). In *Drosophila*, Nct might stabilize PS fragments (Hu et al., 2002; Lopez-Schier and Johnston, 2002) and seems to be involved in transport of PSs to the cell surface (Chung and Struhl, 2001). These results suggested to us that a small, but biologically active, fraction of PS bound to Nct could be released from the ER and targeted to the cell surface, where it interacts with the γ-secretase substrates. We therefore investigated the subcellular localization of PS1 and its binding partner Nct. Indeed we found PS1 on the plasma membrane (PM). We also found that PS1 binds to mature, cell surface–localized Nct. Moreover, inactivation of PSs by mutagenesis of the critical aspartates or treatment with γ-secretase inhibitors affected cell surface reinternalization and PM accumulation of βAPP. Our data suggest that a PS1–Nct complex is released from the ER and transported to late Golgi compartments and the cell surface, where it is biologically active.

Results

Expression of functional EGFP-tagged presenilin

To prove if PSs can reach the PM, we chose an approach that is highly sensitive and independent of fixation methods and antibody affinity. We tagged PS1 and a previously characterized nonfunctional PS1 D385N (Steiner et al., 1999c; Wolfe et al., 1999b) derivative with EGFP. The EGFP cassette was inserted into the large cytoplasmic loop within a region previously shown to be irrelevant for PS function in γ-secretase activity (Saura et al., 2000; Fig. 1 A). The cDNA constructs, PS1–EGFP (PE) and PS1 D385N–EGFP (PEASP) were stably transfected into human embryonic kidney (HEK) 293 cells expressing Swedish mutant βAPP (Citron et al., 1992). Selected cell lines were then investigated for the functional/nonfunctional expression of PE and PEASP. We first analyzed if the fusion proteins could still replace endogenous PS1 and PS2, a phenomenon closely associated with PS stabilization and complex formation (Thinakaran et al., 1997). Consistent with previous results (Thinakaran et al., 1997), expression of PE and PEASP fully replaced endogenous PS1 and PS2 without allowing robust overexpression (Fig. 1 B; for calculation of overexpression see Materials and methods).

As endogenous PS1 (Thinakaran et al., 1996), PE undergoes endoproteolysis and an ∼50-kD CTF (PE_{CTF}) is generated (Fig. 1 B). The molecular mass of this fragment corresponds to the molecular mass of the authentic $PS1_{CTF}$ (∼20 kD) plus the fused EGFP (∼30 kD). In contrast, PEASP does not undergo endoproteolysis and accumulates as a full-length protein (Fig. 1 B), as shown previously for the PS1 D385N mutation (Steiner et al., 1999a; Wolfe et al., 1999b). We next investigated if PE allows normal Aβ production and if PEASP blocks γ-secretase activity. As shown in Fig. 1 C, Aβ production in cells expressing PE or endogenous PS1/PS2 is very similar. In contrast, PEASP significantly reduces Aβ production as expected (Fig. 1 C). Reduced Aβ production is accompanied by the accumulation of βAPP CTFs (De Strooper et al., 1998; Wolfe et al., 1999b), which are the immediate substrates for γ-secretase cleavage. Whereas these fragments accumulate in cells expressing PEASP, very low levels of βAPP CTFs are observed in cells expressing PE and cells expressing endogenous PS1 (Fig. 1 C). If PE is functionally like PS1 wild type (wt), it is expected to promote Aβ production in an Aβ40/42 ratio of ∼9:1 (Selkoe, 1999). Separation of Aβ40 and 42 species secreted by PE-expressing cells shows the expected ratio (Fig. 1 D). Inserting the FAD-associated L166P mutation into PE leads to dramatically increased Aβ42 generation (Fig. 1 D). A similar effect on Aβ40/42 ratio is also observed when this mutation is inserted in PS1 wt (Möhlmann et al., 2002). These experiments clearly indicate that the insertion of EGFP does not affect the physiological function of PS, whereas single point mutations at critical residues abolish (in the case of D385N) or modify
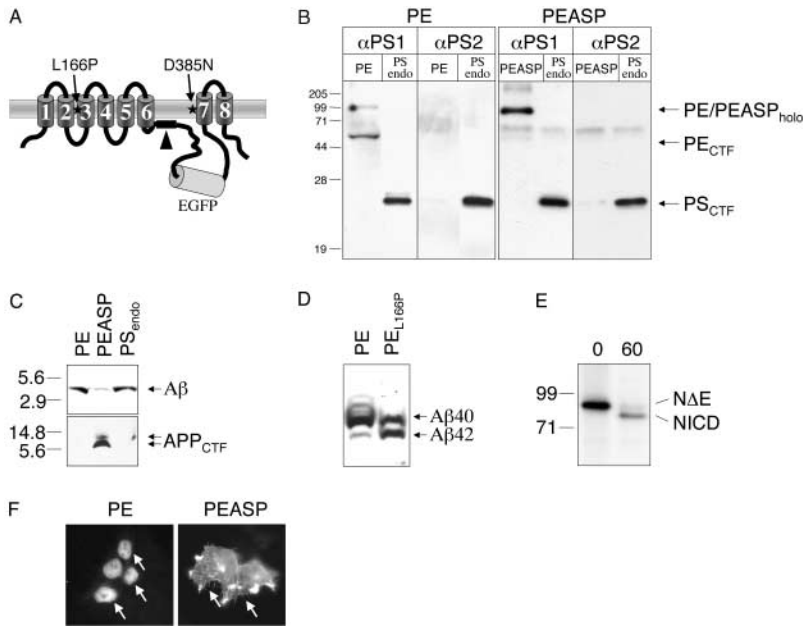
Figure 1. **EGFP-tagged PS1 is fully functional.**
(A) Schematic diagram of EGFP-tagged PS1 variants. EGFP was cloned at codon 351 into the large cytoplasmic loop of human PS1. The endoproteolytic cleavage site within the region coded by exon 9 (black box) is indicated by an arrowhead, and the positions of the critical aspartate at position 385 (mutated in PEASP) and the FAD-associated L166P mutation (mutated in PE L166P) by asterisks. (B) PE and PEASP replace endogenous PS1 and PS2. HEK293 cells stably expressing Swedish βAPP and PE (left) or PEASP (right) or endogenous PS1 and PS2 (PS endo) were analyzed for PS expression by a combined immunoprecipitation/immunoblotting protocol using antibodies 3027/BI.3D7 (for PS1) and 3711/BI.HF5c (for PS2). Molecular weight markers in kD are indicated on the left, positions of holoprotein and CTFs are indicated on the right. Note that PE and PEASP replace endogenous PS. (C) γ-Secretase function is normal in cells stably expressing PE, but greatly reduced in cells stably expressing PEASP. Media and lysates of cells stably expressing Swedish βAPP and PE or PEASP or endogenous PS (PS$_{endo}$) were collected, separated on Tris/Tricine gels, blotted on nitrocellulose membrane, and probed with antibody 6E10 (Aβ) or 6687 (APP$_{CTF}$). (D) The ratio of Aβ 40/42 is not altered by the EGFP tag. Media of cells stably expressing Swedish βAPP and PE (PE) or PE carrying an FAD-associated L166P mutation (PE$_{L166P}$) were collected, immunoprecipitated with antiserum 3926, separated by electrophoresis (Wiltfang et al., 1997), blotted, and probed with antibody 6E10. Aβ 40/42 production is normal in PE-expressing cells, but dramatically changed in PE$_{L166P}$-expressing cells. (E and F) Cells stably expressing PE support Notch cleavage. (E) Cells stably expressing PE and constitutively active NotchΔE (NΔE) were pulse labeled for 15 min with ^{35}S-methionine (0), or pulse labeled for 15 min and chased for 60 min (60). Lysates were immunoprecipitated using antibody 9E10 and analyzed by SDS-PAGE and audioradiography. Molecular weight markers in kD are indicated on the left, the position of NΔE and the γ-secretase–dependent fragment, NICD, are indicated on the right. (F) Cells stably expressing PE or PEASP were transiently transfected with NΔE, fixed, and processed for immunofluorescence using antibody 9E10. In PE cells, staining is seen in the nucleus (arrows), indicating efficient Notch cleavage and translocation of NICD, whereas in PEASP cells myc staining is seen on the PM, showing that Notch cleavage is blocked (arrows mark stained filopodia, indicative of PM).

(in the case of L166P) the function of EGFP-tagged PS1 in a predicted manner. To further prove functional expression of PE, we also analyzed Notch endoproteolysis and nuclear translocation of the Notch intracellular domain (NICD). As shown in Fig. 1 E, NICD is produced in cells expressing PE and NotchΔE, a constitutively active Notch construct (Schroeter et al., 1998). In addition, we observed efficient nuclear translocation of Notch derivatives exclusively in cells expressing PE, but not in cells expressing PEASP (Fig. 1 F). In the latter case, NotchΔE accumulates on the PM (Fig. 1 F, right). Taken together, these data demonstrate that expres-

sion of an EGFP-tagged PS1 does not interfere with its physiological and pathological functions. Moreover, these findings suggest that exogenous PS is delivered to the subcellular compartments, where endogenous PS is active (for the analysis of PM trafficking of endogenous PS see below).

Detection of presenilin on the cell surface of living cells

We investigated the subcellular distribution of PE using live cell microscopy. Two different planes of focus are shown in Fig. 2, A and B, respectively, and enlargements of the boxed areas are shown in Fig. 2, C–G. PE staining can be clearly seen in
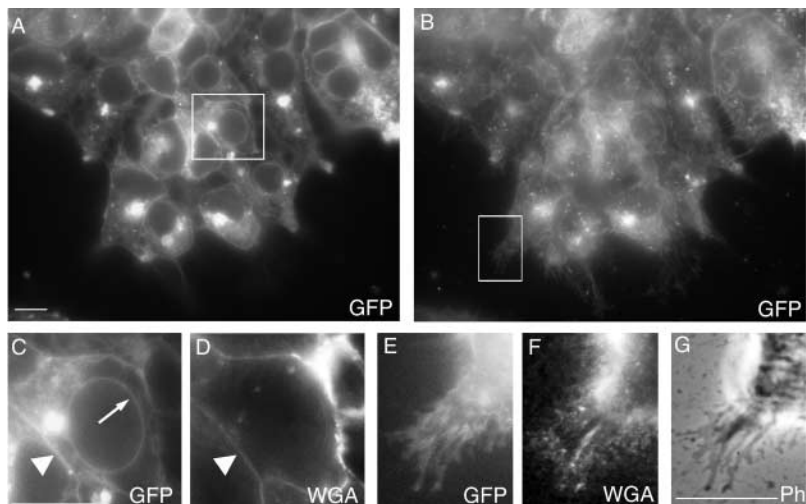
Figure 2. **PE is on the surface of living cells.** HEK293 cells stably expressing Swedish βAPP and PE were grown on poly-L-lysine–coated coverslips, labeled with TRITC–WGA, mounted for live imaging, and imaged with a sensitive CCD camera. A and B show two different focal planes of a set of living cells, and C–G show enlargements of the boxed areas. Note the PE staining in the nuclear envelope (A and arrow in C), the borders of neighboring cells (arrowheads in C and D), and on pseudopod-like processes (E–G). Ph, phase contrast. Bars, 10 μm.

Figure 3. **PEASP is on the surface of living cells.**
Cells stably expressing PEASP were grown on poly-
L-lysine–coated coverslips, labeled with TRITC–
WGA, mounted for live imaging, and imaged with
a sensitive CCD camera. A and B show two different
focal planes of a set of living cells, and C–E show
enlargements of the boxed area. Note the PEASP
staining of the nuclear envelope and vesicular
structures (A), and of pseudopod-like processes (C–E,
arrows). Ph, phase contrast. Bars, 10 μm.
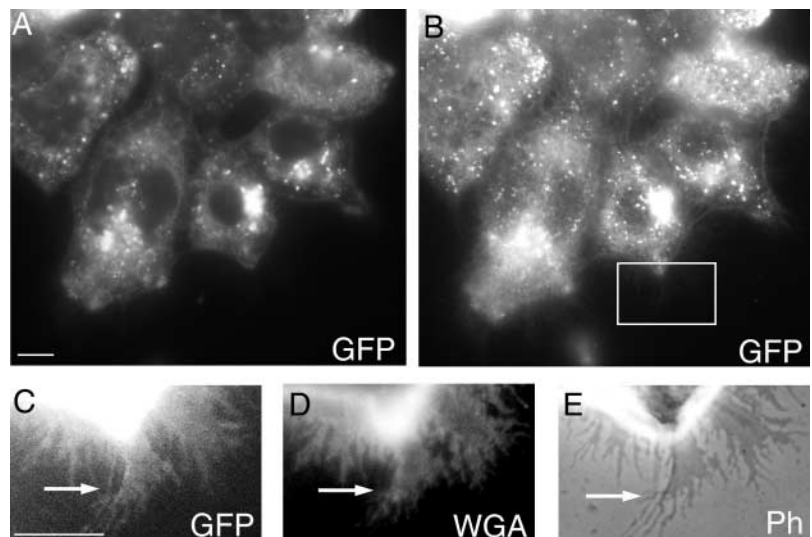
the nuclear envelope, vesicular structures, and an ER-like net-
work. Surprisingly, the borders of neighboring cells (Fig. 2 C),
marked by staining with fluorescent WGA (TRITC–WGA;
Fig. 2 D) were clearly labeled, suggesting a PM localization of
PE. Another example of surface localization is shown in Fig. 2,
E–G, where a lamellipodium (indicated by phase contrast in
Fig. 2 G) of a cell is labeled with PE (Fig. 2 E) as well as
TRITC–WGA (Fig. 2 F). The observed PM localization of PE
is not an artifact of our detection method, because ER-retained
GFP–KDEL does not show PM staining under identical imag-
ing conditions (Fig. S1, available at http://www.jcb.org/cgi/
content/full/jcb.200201123/DC1).

PEASP was also detected on the PM (Fig. 3, A and B). As
compared with PE, a more prominent staining of the vesicu-
lar structures was observed (compare Fig. 2, A and B, with
Fig. 3, A and B). Most of these vesicular structures can be
stained with lysotracker and antibodies against lamp-2, sug-
gesting that they are endosomes/lysosomes (unpublished
data). However, PEASP is also located in lamellipodia, as

demonstrated in the enlargements, where the focal plane of
attachment to the coverslip is shown (Fig. 3 C). Again, fine
cellular processes shown in the phase image (Fig. 3 E) are la-
beled with PEASP (Fig. 3 C) and TRITC–WGA (Fig. 3 D).

To further prove that significant amounts of PE and
PEASP are on the PM, we performed total internal reflection
microscopy (TIRM). This technique selectively excites fluoro-
phores near the coverslip, whereas fluorophores >100 nm
away (and deeper in the cell) are not excited. Therefore, only
the area where the cell attaches to the coverslip is illuminated,
and obscuring fluorescence from internal structures is dimin-
ished (for review see Toomre and Manstein, 2001). We per-
formed TIRM on living PE- or PEASP-expressing cells (Fig.
4). The TIRM images on the left show the PM of both PE
and PEASP cells, best visible in the lamellipodia indicated by
arrows. Both PE and PEASP show a similar degree of PM
staining. The pronounced vesicular staining observed for
PEASP (compare Figs. 2 and 3) is also visible to some extent
in the TIRM image, suggesting that some of these vesicles are

Figure 4. **Cell surface localization of PE and
PEASP visualized by TIRM.** Living cells stably
expressing PE or PEASP and grown in poly-L-
lysine–coated glass bottom dishes were imaged
using TIRM on the left or using conventional
epifluorescence (epi) on the right. Arrows indicate
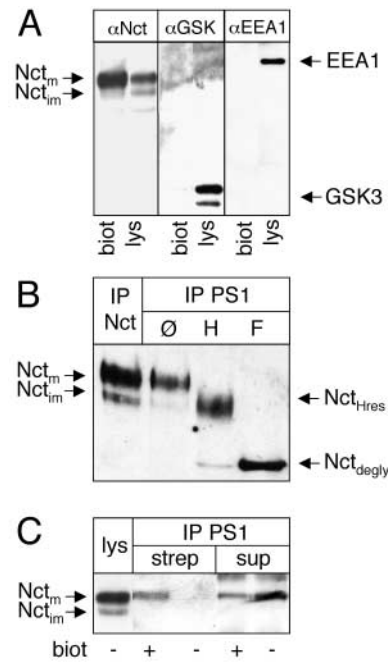labeled lamellipodia and filopodia, indicative of
PM. Bar, 10 μm.
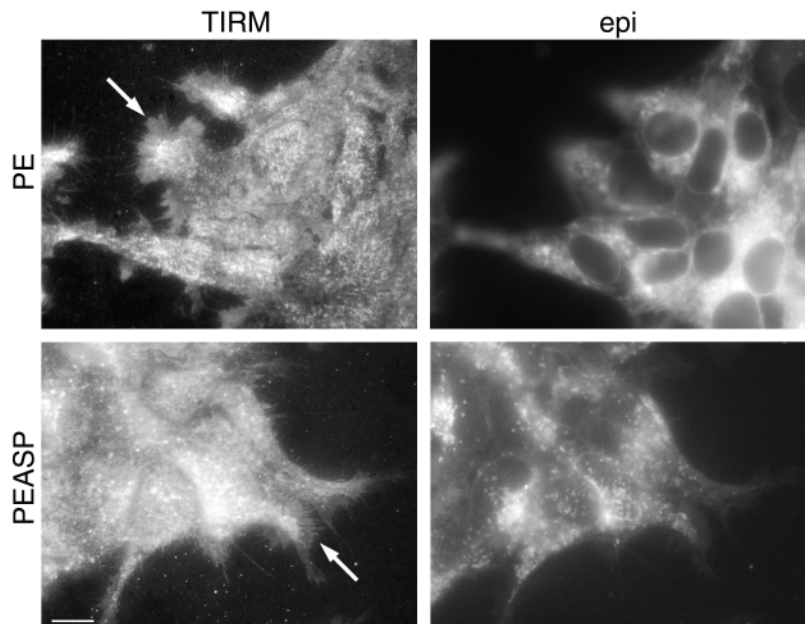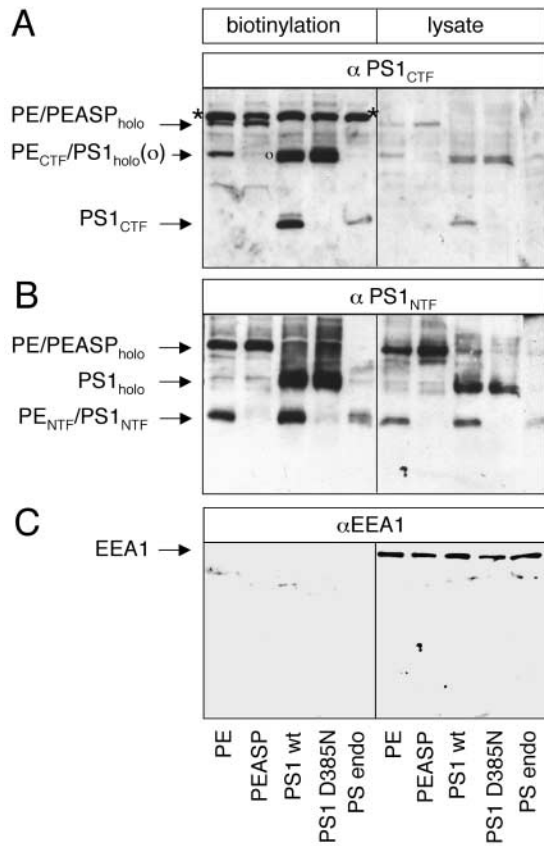
Figure 5. **PS1 can be biotinylated at the cell surface.** HEK293 cells stably expressing Swedish βAPP and PE, PEASP, PS1 wt, PS1 D385N, or endogenous PSs were surface biotinylated. After streptavidin precipitation, biotinylated proteins and cell lysates (1/60 of total) were separated using SDS-PAGE, blotted, and probed for PS1 CTF (A), and stripped and reprobed for PS1 NTF (B). Note that PE CTF and PS1 holoprotein (o) have similar molecular weights. Asterisks indicate unspecific background bands. To control for intactness of cells during the biotinylation, the blot was stripped and reprobed for EEA1 (C). No EEA1 staining can be detected on the streptavidin-precipitated material (left, biotinylation), whereas cell lysates contain robust amounts of EEA1 (right, lysate).


Figure 6. **Mature Nct interacts with endogenous PS at the PM.** (A) HEK293 cells expressing endogenous PSs and endogenous Nct were surface biotinylated, lysed, separated using SDS-PAGE, blotted, and probed for Nct. Biot, streptavidin-Sepharose precipitation; lys, 1/100 of cell lysate; Nct_{im}, immature Nct; Nct_m, mature Nct. To control for intactness of cells during the biotinylation, the blot was stripped and reprobed for GSK-3 (αGSK), and stripped and reprobed for EEA1 (αEEA1). Neither GSK-3 nor EEA1 staining can be detected on the streptavidin-precipitated material (biot), whereas cell lysates contain robust amounts of GSK-3 and EEA1 (lys). The GSK antibody is reactive with GSK-3α (upper band) and GSK-3β (lower band). Identical results were obtained from cells expressing exogenous PS1 wt (unpublished data). (B) Coimmunoprecipitation of endogenous PS1 and mature Nct. HEK293 cells expressing endogenous Nct and PSs were lysed in 2% CHAPS, and immunoprecipitated with an Nct antibody (IP Nct) or PS1 antiserum 3027 (IP PS1). Immunoprecipitates were digested with endoH (IP PS1, H) or N-glycosidase F (IP PS1, F). (C) Coimmunoprecipitation of endogenous PS1 and biotinylated endogenous Nct. HEK293 cells expressing endogenous Nct and endogenous PSs were subjected to surface biotinylation with (+) or without (−) biotin. Membrane fractions were prepared, lysed in 2% CHAPS, immunoprecipitated with antiserum 3027 against PS1 CTF, eluted, and the eluate was precipitated with streptavidin-Sepharose (strep). Samples were separated on SDS-PAGE together with a control cell lysate (lys) and 15 μl of the streptavidin-Sepharose supernatants (sup). Blots were probed with the Nct antibody. Note that the supernatant of the biotinylated lysate contains less Nct because biotinylated Nct was streptavidin precipitated. Nct_{im}, immature Nct; Nct_m, mature Nct; Nct_{Hres}, endoH-resistant Nct; Nct_{degly}, deglycosylated Nct.

very close to the PM. Right panels show conventional epifluorescence of the same cells. As a control, we performed TIRM on living HEK293 cells stably expressing GFP–KDEL. No staining of the PM could be detected under identical imaging conditions (Fig. S2). Taken together, these data suggest that significant amounts of PS1 are located at the PM.

Although we clearly demonstrated that the EGFP-tagged PS derivatives showed the expected functional properties, we performed further experiments with untagged PS1 to support the above described data with direct biochemical evidence. In addition, we also analyzed PM targeting of endogenous PSs. Cell lines expressing endogenous PSs, PE, PEASP, PS1 wt, or PS1 D385N (Steiner et al., 1999c) were biotinylated at 4°C. Biotinylated proteins were isolated and PSs were detected by immunoblotting using antibodies to the COOH and NH$_2$ termini, respectively. As shown in Fig. 5, we detected biotinylated PE_{CTF}, NH$_2$-terminal fragment of PE (PE_{NTF}), PE, and PEASP holoprotein, $PS1_{CTF}$ and $PS1_{NTF}$ as well as PS1 holoprotein, suggesting that all PS derivatives were at the PM. Importantly, endogenous $PS1_{NTF}$

and $PS1_{CTF}$ can be biotinylated at the PM (Fig. 5). Because endogenous PS holoprotein is efficiently processed to $PS1_{NTF}$ and $PS1_{CTF}$ (Thinakaran et al., 1996), it could not be detected by biotinylation. Moreover, the ratio of surface/internal PS of roughly 1/30 is not changed upon overexpression of PS derivatives (see Materials and methods). This strongly indicates that overexpression of PS does not change its subcellular distribution. As a control for selective cell surface biotinylation, we immunoblotted the isolated biotinylated proteins with an antibody to early endosomal autoantigen 1 (EEA1; a protein localized to early endosomes). As

Figure 7. **Endocytosis of βAPP, but not BACE, is delayed in cells expressing nonfunctional PS1.** HEK293 cells stably expressing Swedish βAPP and PS1 wt or PS1 D385N were incubated on ice with antiserum 5313, washed, and chased at 37°C. Cells shown in the third row were additionally treated for 4 h with DAPT. Cells stably expressing BACE were incubated on ice with antiserum 7523, washed, and chased at 37°C. After the indicated time points, cells were fixed and processed for immunofluorescence. Bar, 10 μm.
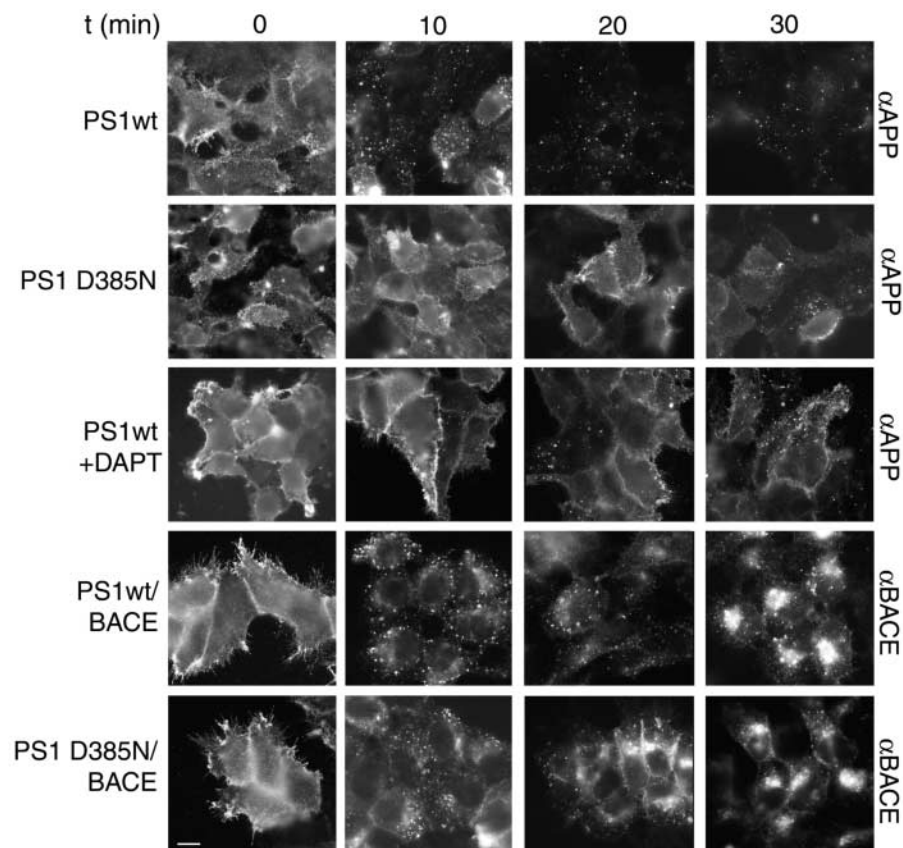
expected, no biotinylated EEA1 was observed, although the investigated cell lines express significant amounts of this intracellular protein (Fig. 5, bottom).

## A PS1–Nct complex is targeted to the PM

An additional line of evidence for cell surface trafficking of PS1 was obtained by the analysis of the PS1 binding protein Nct. Nct is an essential component of the PS complex, and is required for γ-secretase activity (Yu et al., 2000; Chung and Struhl, 2001; Levitan et al., 2001; Edbauer et al., 2002; Hu et al., 2002; Lopez-Schier and Johnston, 2002). We therefore analyzed Nct trafficking through the secretory pathway and its interaction with PS1. Importantly, the entire analysis was performed with cells expressing endogenous PSs and Nct. Endogenous Nct is present predominantly in a mature and, to a lesser extent, an immature form (Fig. 6 A, αNct, lys). Cell surface biotinylation demonstrated that the mature form is present on the PM, demonstrating that Nct can leave the ER only upon full maturation (Fig. 6 A, αNct, biot). Cells were intact during the biotinylation, as indicated by reprobing the blot with antibodies against glycogen synthase kinase 3 (GSK-3) and EEA1 (Fig. 6 A, αGSK, αEEA1). To analyze if immature or mature Nct interacts with PS1, we performed a coimmunoprecipitation of Nct with PS1 antibodies followed by deglycosylation (Fig. 6 B, IP PS1). As a control, cell lysates were immunoprecipitated using Nct antibodies (Fig. 6 B, IP Nct). Immunoprecipitation with PS1 antiserum 3027 preferentially coprecipitates mature Nct (Fig. 6 B, ∅). The coimmunoprecipitated Nct is endoH resistant, as digestion with endoH leads only to a minor shift to higher mobility (Fig. 6, B and H). This minor

shift is most likely explained by incomplete glycosylation of some of the many N glycosylation sites (Leem et al., 2002). In contrast, the immature form of Nct is shifted upon endoH digestion to the position of the totally deglycosylated Nct (Fig. 6 B, lanes H and F). These data demonstrate that endogenous PS1 bound to endogenous Nct reached late Golgi compartments, where complex glycosylation occurs.

We next analyzed whether the PS1–Nct complex is targeted to the cell surface. To this end, we performed surface biotinylation followed by coimmunoprecipitation of Nct using PS1 antibodies. Bound proteins were eluted, subjected to streptavidin-Sepharose precipitation, and detected using Nct antibodies (Fig. 6 C). Indeed, biotinylated mature Nct was coimmunoprecipitated with PS1 (Fig. 6 C, strep$^+$). No Nct was detected when the biotin was omitted (Fig. 6 C, strep$^-$). The supernatant of the streptavidin-Sepharose precipitation showed that Nct was coimmunoprecipitated with or without biotin (Fig. 6 C, sup). These results demonstrate that PS1 and Nct are present in a complex at the PM.

Functional inactivation of presenilin affects trafficking of cell surface βAPP

After demonstrating targeting of a PS1–Nct complex to the PM, we wanted to investigate whether inactivation of PS would also affect cellular mechanisms other than Aβ production. To this end, we investigated endocytosis of βAPP in living cells expressing either fully functional PS1 or the nonfunctional PS1 D385N mutant. Cells expressing either PS1 wt or PS1 D385N (Fig. 7) were incubated on ice with antiserum 5313 recognizing the ectodomain of βAPP, washed, and returned to 37°C. After the indicated time points, cells
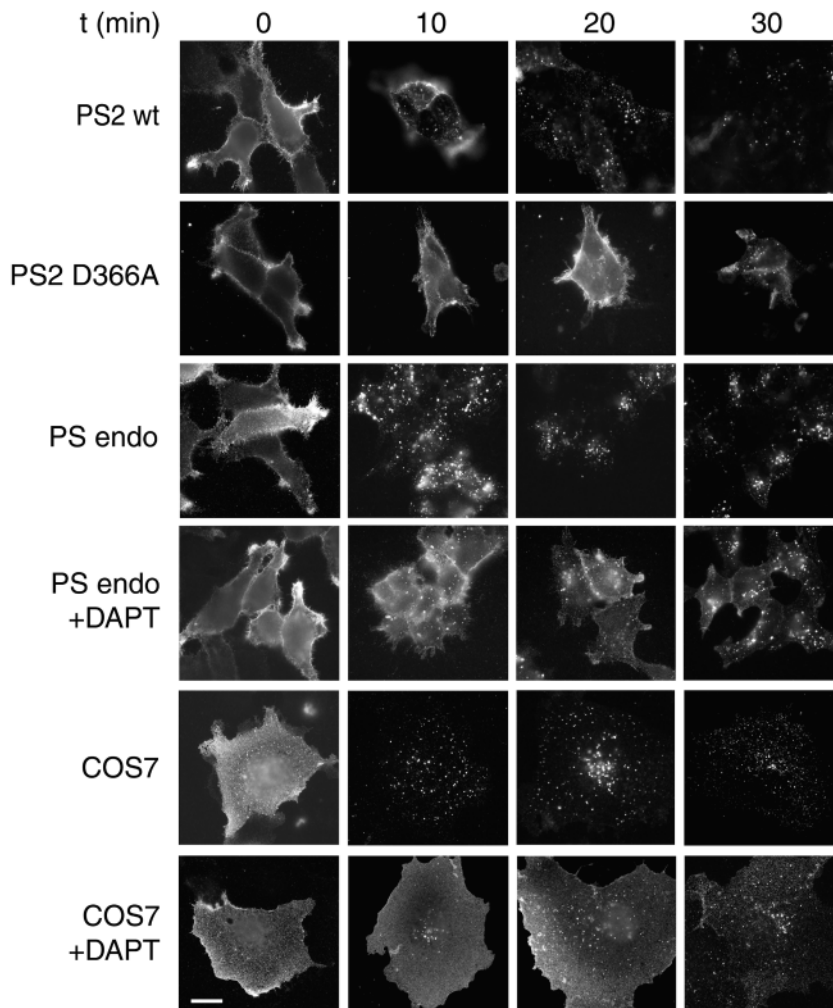
Figure 8. **Endocytosis of βAPP is delayed in cells expressing nonfunctional PS2 or endogenous PSs.** HEK293 cells stably expressing Swedish βAPP and PS2 wt or PS2 D366A, and HEK293 cells expressing βAPP$_{695}$ and endogenous PS1 and PS2 (PS endo) as well as COS7 cells transiently transfected with βAPP$_{695}$ (COS7) were incubated for 4 h in the presence or absence of DAPT. Thereafter, they were incubated on ice with antiserum 5313, washed, and chased at 37°C. After the indicated times, cells were fixed and processed for immunofluorescence. Bar, 10 μm.

were fixed and processed for immunofluorescence. In PS1 wt–expressing cells, cell surface βAPP was completely taken up after 10 min (Fig. 7). In contrast, βAPP was present much longer on the surface of cells expressing PS1 D385N. After 10 min at 37°C, an unchanged surface staining of βAPP was observed and there were no endocytic structures containing βAPP. Only after 20–30 min did βAPP-containing endocytic structures become visible, but no complete uptake was observed at these time points (Fig. 7).

Next we tested if other βAPP interacting type I transmembrane proteins are also delayed in reinternalization upon the expression of functionally inactive PS1 D385N. We investigated endocytosis of BACE, a molecule previously shown to be reinternalized from the cell surface (Huse et al., 2000; Walter et al., 2001). This revealed that endocytosis of BACE was not affected (Fig. 7), indicating that inactivation of PS1 does not have a general effect on the endocytosis of proteins involved in βAPP metabolism.

To further prove that inactivation of a PS-dependent γ-secretase activity affects reinternalization of βAPP, we used the highly specific γ-secretase inhibitor DAPT (Dovey et al., 2001). Incubation of cells with DAPT leads to biochemical phenotypes very similar to those observed in PS1 D385N–expressing cells (Dovey et al., 2001; Sastre et al., 2001), i.e., inhibition of Aβ and βAPP intracellular domain production, enrichment of βAPP CTFs, and inhibition of NICD genera-

tion accompanied by a lack of Notch signaling (Geling et al., 2002). Cells expressing PS1 wt were incubated for 4 h with DAPT and processed for βAPP uptake as above. Endocytosis of βAPP was delayed, and significant levels of surface βAPP were still present at the PM after 10 min at 37°C. After 20 and 30 min at 37°C, most of the βAPP had been endocytosed, however, at all time points, there were cells present with surface-retained βAPP (Fig. 7). Similar, albeit weaker, effects were observed using a different γ-secretase inhibitor (Li et al., 2000b; unpublished data). These data therefore demonstrate that functional inactivation of a PS1-associated γ-secretase activity not only affects βAPP processing but also its trafficking from the cell surface to endosomes.

The delay in endocytosis was also observed in cells expressing functionally inactive PS2 D366A, demonstrating similar activities of nonfunctional PS1 and PS2 (Fig. 8). Importantly, inactivation of endogenous PSs with DAPT resulted in a delayed endocytosis of βAPP, very similar to the results observed with PS-transfected cells (Fig. 8). βAPP-expressing HEK293 and COS7 cells were incubated in the presence or absence of DAPT and processed for βAPP uptake as above (Fig. 8). In both cell lines, the inactivation of endogenous PSs resulted in delayed endocytosis of βAPP, fully reproducing the findings observed in transfected cells.

If reinternalization of βAPP is delayed, one should obtain elevated levels of cell surface βAPP in cells expressing the non-

functional PS1 D385N variant. To prove this, we surface biotinylated βAPP. Biotinylated βAPP was quantified using ^{125}I-labeled secondary antibodies. Consistent with previous data (Kim et al., 2001), PS1 D385N–expressing cells showed 2.8 ± 1 ($n = 8$) times more βAPP on the surface than cells expressing PS1 wt. This suggests that indeed βAPP accumulates on the cell surface, probably due to delayed reinternalization.

Loss of PS function, but not FAD mutants or uncleavable PS mutants, affects reinternalization of βAPP

The above-described results suggest that a loss or reduction of PS function is responsible for the observed reduction of βAPP reinternalization. To prove if a gain of misfunction, which apparently is caused by all FAD mutations, affects surface metabolism of βAPP, we analyzed two FAD-associated PS mutations. We chose the PS1 G384A mutation, because this mutant shows an exceptional 5.5-fold increase of Aβ42 generation (Steiner et al., 2000). In addition, we also included the PS1 ΔE9 mutation, because that produces high Aβ42 levels, but in addition accumulates as an uncleaved holoprotein (like the PS1 D385N and PS2 D366A mutants) (Thinakaran et al., 1996). Because the PS1 ΔE9 may mimic a cleaved PS derivative (Ratovitski et al., 1997; Capell et al., 1998; Steiner et al., 1999b), we also investigated a previously characterized PS1 M292D point mutation, which inhibits endoproteolysis (Steiner et al., 1999c). Expression of any of these PS variants allowed normal uptake of βAPP, suggesting that a loss or reduction of PS function, but not a gain of pathological function, is responsible for the observed defects in endocytosis (Table I).

Discussion

The functional role of PSs in γ-secretase cleavage of βAPP is currently unclear. Two controversial models are discussed. The first model suggests that PSs contribute the catalytically active sites of a γ-secretase complex or at least an essential cofactor of it (Wolfe et al., 1999b; Wolfe and Haass, 2001). In the second model, an indirect role of PSs in trafficking, rather than processing, of βAPP is assumed (Kim et al., 2001). Support for the latter comes from studies that demonstrate that βAPP and βAPP CTFs are enriched on the surface of cells expressing functionally inactive PS (Capell et al., 2000a; Kim et al., 2001). Moreover, the subcellular distribution of PSs apparently does not overlap with the cellular sites of γ-secretase activity in late compartments at or close to the cell surface, a finding that created the so-called spatial paradox (Annaert et al., 1999; Checler, 2001; Cupers et al., 2001). This model implies that PSs are required to release γ-secretase activity from early transport compartments, but in its ultimate consequence predicts a γ-secretase complex, which functions without physical contact to PS.

Considering these two contradictory models, we first reevaluated the cellular distribution of PS1. Endogenously as well as exogenously expressed PS1 was biochemically detected on the PM. Moreover, we found that γ-secretase activity and PS1 codistributed in a post trans-Golgi compartment in MDCK cells (unpublished data). Furthermore, we could clearly demonstrate that an EGFP-tagged PS1 localizes on the PM in living cells. It is highly unlikely that the fusion of the EGFP domain changed trafficking of PS1, because we could demonstrate that such PS derivatives are fully functional and can be inactivated by the introduction of the D385N mutation as expected. Independent support for a PM localization of PS1 comes from the coimmunoprecipitation of Nct with PS1. Preferentially mature, fully glycosylated Nct associates with PS1, indicating that a PS1–Nct complex is targeted to a post-Golgi compartment. Like PS1, a fraction of Nct can be biotinylated at the PM. Moreover, biotinylated endogenous Nct could be coimmunoprecipitated with endogenous PS1, strongly suggesting that a PS1–Nct complex is located at the PM.

In addition to our findings on PS localization in a late Golgi compartment and at the cell surface, we found that inactivation of both endogenous and exogenous PS function affects the endocytosis of βAPP from the PM. Therefore, it appears likely that PSs have a dual function in trafficking and processing. Based on a quantitative analysis, we calculated that ~1/30 of total PS is located on the PM. From these data, we conclude that rather small amounts of PSs could indeed exert a biological activity at or very close to the PM. It is not known how much active PS complex is needed for functional γ-secretase activity. However, assuming a catalytic activity of the complex, the amounts of PS1 we found on the PM could well account for the cleavage of βAPP, Notch, ErbB4, E-cadherin, and LDL receptor-like protein and other so far unidentified γ-secretase substrates. Our data on the surface localization of PS1 are therefore in full accordance with PSs being part of the proteolytically active γ-secretase complex.

It is unclear why conventional immunolabeling techniques did not allow the detection of PSs beyond the intermediate Golgi apparatus. However, GFP fluorescence in our constructs is rather weak, suggesting low expression levels, and thus sensitive detection methods are required to visualize PS. In agreement with previous reports (Walter et al., 1996; De Strooper et al., 1997; Annaert et al., 1999; Cupers et al., 2001), in our hands, most of PS seems to be located in the ER, sometimes masking the weak staining on the PM. It is also important to note that upon fixation, the GFP fluorescence is significantly reduced (unpublished data), which makes the detection of surface PS very difficult.

Our data demonstrate that trafficking of βAPP is altered in cells expressing nonfunctional PS1, whereas the traffick-

Table I. Endocytosis of APP in cell lines expressing different PS variants

Cell line	DAPT$^-$	DAPT$^+$
HEK293/APPswe/PS1 wt	N	D
HEK293/APPswe/PS1 D385N	D	
HEK293/APPswe/PS2 wt	N	
HEK293/APPswe/PS1 D266A	D	
HEK293/APPswe/PS endo	N	D
HEK293/APP/PS endo	N	D
COS7/APP	N	D
HEK293/APPswe/PS1 G384A	N	
HEK293/APPswe/ PS1 ΔE9	N	
HEK293/APPswe/PS1 M292D	N	

APP uptake experiments were performed as described in Fig. 7. APPswe, Swedish APP; D, delayed endocytosis; N, normal edocytosis.

ing of another βAPP processing enzyme, BACE, is unaffected. The accumulation of βAPP CTFs on the surface (Capell et al., 2000a; Kim et al., 2001) could simply reflect accumulation of the precursor of γ-cleavage, because this cleavage is blocked. However, accumulation of full-length βAPP on the surface indicates an effect on trafficking, independent of the role of PSs in γ-secretase function (this study; Kim et al., 2001). The cellular mechanism responsible for the surface accumulation of βAPP could be the delayed reinternalization due to the saturation by the accumulation of APP and its derivatives on the PM. Indeed, we found that βAPP endocytosis is slowed down in cells expressing nonfunctional PS1 or PS2, which would lead to an accumulation of surface βAPP if exocytic transport is unaltered. In line with unaltered exocytosis, it has been shown that maturation of βAPP is not affected in cells expressing nonfunctional PS1 (Wolfe et al., 1999b).

Taken together, our data demonstrate that a small, but functionally active, fraction of PS1 bound to Nct is released from the ER and targeted to the PM. In agreement with the spatial paradox, the majority of PS1 is retained within the ER, where little γ-secretase activity is observed. However, in clear contrast to the proposals of the spatial paradox, a fraction of PS1 (bound to Nct) is located within a post-Golgi compartment and at the PM. A function of PS on the cell surface is supported by our finding that inactivation of PSs by two independent methods slows endocytosis of βAPP from the PM. The loss of PS function may indirectly affect βAPP uptake due to a toxic gain of misfunction. This is supported by our previous finding that the aspartate mutants of PS cause a massive accumulation of βAPP CTFs (Capell et al., 2000a), which cannot only be explained by the loss of γ-secretase activity, but rather by reduced degradation. The latter may very well be due to reduced endosomal/lysosomal targeting of the βAPP CTFs, resulting in their accumulation on the cell surface (Capell et al., 2000a; Kim et al., 2001).

Our data suggest a dual function for PSs: they may be involved in the trafficking of βAPP, via so far unidentified mechanisms, and in the γ-secretase processing of βAPP by providing the catalytically active sites within the γ-secretase complex. Both functions are apparently related to the formation of a PS–Nct complex, which may contain other additional subunits, such as aph-1 (Goutte et al., 2002). In fact, absence of Nct (Yu et al., 2000; Chung and Struhl, 2001; Levitan et al., 2001; Edbauer et al., 2002; Hu et al., 2002; Lopez-Schier and Johnston, 2002) and aph-1 (Goutte et al., 2002) severely affects γ-secretase activity.

Materials and methods

Antibodies and cell lines
Antiserum 7523 against the NH2 terminus of BACE was described before (Capell et al., 2000b). Aβ, βAPP, and βAPP CTFs were detected using antibodies 3926/6E10 (Sastre et al., 2001), 5313, and 6687 (Steiner et al., 2000), respectively. The PS1 CTF was immunoprecipitated with antiserum 3027 and detected with monoclonal BI.3D7 or 3027 as previously described (Steiner et al., 1999b). The PS1 NTF was detected using the monoclonal PS1 N antibody (provided by R. Nixon, Nathan Kline Institute, Orangeburg, NY). The PS2 CTF was immunoprecipitated with antiserum 3711 and detected with monoclonal BI.HF5c as previously described (Capell et al., 1998). EEA1 was detected using the monoclonal EEA1 antibody (Sigma-Aldrich). NotchΔE (Schroeter et al., 1998) and NICD were detected using monoclonal 9E10 antibody (Santa Cruz Bio-

technology, Inc.). Nct was detected using polyclonal anti-Nct COOH-terminal antibody (Sigma-Aldrich). GSK-3 was detected using monoclonal antibody against GSK-3β (Santa Cruz Biotechnology, Inc.). HEK293 cells stably expressing Swedish mutant βAPP (Citron et al., 1992) and PS1 wt, PS1 D385N, PS2 wt, or PS2 D266A were described before (Steiner et al., 1999a,c). HEK293 cells stably expressing Swedish mutant βAPP and PS1 wt or PS1 D385N were transfected with BACE cDNA in pcDNA3.1/Hygro+ (Invitrogen) and pools of stably expressing cells were selected.

cDNA constructs, transfections, and screening of stably transfected cell lines
To generate an EGFP-tagged PS, a NotI restriction site was introduced between codon 351 and 352 of the cytoplasmic loop of human PS1, resulting in PS1not. EGFP cDNA was then fused in-frame into the PS sequence using the NotI site. Introduction of the NotI site results in two additional glycine codons at NH2 and COOH termini of EGFP, respectively. Proper orientation of EGFP was checked by transfecting miniprep DNA into COS7 cells and analyzing GFP fluorescence. One clone, PE, was subcloned in pCDNA3.1Zeo (Invitrogen). PS1 D385N–EGFP and PS1 L166P–EGFP were generated by mutagenizing PE with appropriate oligonucleotides using QuikChange Site-Directed Mutagenesis Kit (Stratagene). The former construct was called PEASP, the latter PE (L166P).

For transient or stable transfection, Fugene (Roche) was used. HEK293 cells stably expressing Swedish βAPP were transfected with PE or PEASP or PE (L166P) and clones were selected for stable integration. Several clones expressing each construct were analyzed and one representative clone was chosen for further analysis. PE17 was the clone used for analysis of PE, and PEASP1 was the one used for PEASP. For analysis of Notch processing, PE 17 cells were transfected with NotchΔE/pcDNA3.1/Hygro+, and a pool of stably expressing cells was obtained by selection with hygromycin. Alternatively, PE 17 cells were transfected and processed for immunofluorescence the following day.

As a control for microscopy, HEK293 cells were transiently transfected with pEF/myc/ER/GFP (Invitrogen), coding for a GFP–KDEL. For APP uptake experiments, COS7 cells were transiently transfected with βAPP695.

Quantitation of expression levels of exogenous PS
For quantitating membrane lysates (Capell et al., 1998) and total lysates of HEK293, cells expressing endogenous PSs or stably expressing PS1 wt or PE were separated on 12% urea gels, blotted, and probed with antiserum 3027. Expression levels were quantitated using ^{125}I secondary antibodies and a phosphoimager system. Total exogenous PS (holoprotein and CTF) was overexpressed 10-fold, compared with endogenous PS1 levels. Only a twofold overexpression of exogenous PS CTF was observed. Because the biologically active PS complex contains the PS fragments (Capell et al., 1998; Li et al., 2000a), this demonstrates a rather low level of overexpression.

Surface biotinylation
HEK293 cells grown on poly-L-lysine–coated 10-cm (for PS and Nct detection) or 6-cm dishes (for APP detection) were washed in ice cold PCM (PBS supplemented with 1 mM CaCl2, 0.5 mM MgCl) and incubated for 30 min on ice in PCM containing 1 mg/ml (for PS and Nct) or 0.5 mg/ml (for βAPP) sulfo-succinimidyl-6-([+]-biotinamido)-hexanoate (Molecular Biosciences). Thereafter, biotinylation was quenched by washing two times in 50 mM NH4Cl–PBS on ice, followed by a 10-min incubation on ice in 50 mM NH4Cl–PBS. In some experiments, 20 mM glycine–PBS was used for quenching. After two additional washes, cells were lysed in STEN lysis buffer (50 mM Tris, pH 7.6, 150 mM NaCl, 2 mM EDTA, 1% NP-40), and biotinylated proteins were precipitated with streptavidin-Sepharose. Biotinylated proteins and 1/60 of total cell lysates were separated on 12% SDS-urea gels (PS) or 8% SDS gels (βAPP and Nct) and blotted onto PVDF membranes. PS1 was detected using antibodies 3027 or PS1 N, Nct using anti-Nct antibody, and βAPP using antiserum 5313. As a control, blots were stripped and reprobed with EEA1 or GSK-3 antibody. Similar blots to those shown in Fig. 5 were incubated with ^{125}I secondary antibodies, and the radioactive signal was detected using a phosphoimager system. The ratio of biotinylated versus total PS was then calculated.

Quantitation of cell surface βAPP
For quantitation of surface βAPP, cells were biotinylated as described above. Biotinylated βAPP was detected using antiserum 5313 and ^{125}I secondary antibody and quantified by phosphoimaging. In each experiment, the values of biotinylated βAPP divided by total βAPP of PS1 wt–expressing cells were set to 1, and the values of biotinylated βAPP divided by total βAPP of PS1 D385N–expressing cells was related to 1.

Coimmunoprecipitation and deglycosylation of Nct

Nct was coimmunoprecipitated from membrane fractions extracted in 2% CHAPS with antiserum 3027 against PS CTF (Capell et al., 1998). EndoH and N-glycosidase F digestion was performed according to the supplier's instructions (Roche). For coimmunoprecipitation and recapture of biotinylated Nct CHAPS lysates from the cell surface, biotinylated cells were immunoprecipitated with antiserum 3027 against PS CTF. Bound proteins were eluted from protein A–Sepharose as described (Bonifacino et al., 2000), and biotinylated proteins were precipitated using streptavidin-Sepharose. Nct was detected using Nct antibody.

Cell surface uptake of βAPP and BACE

Cells plated on poly-L-lysine–coated coverslips were incubated for 4 h in the presence or absence of 250 nM DAPT (provided by Boehringer Ingelheim Pharma KG), washed in ice cold PCM, and incubated on ice in a 1:200 5313 (for βAPP detection) or 7523 (for BACE detection) antibody dilution in PCM. After 20 min, cells were washed in PCM on ice, and then PCM was replaced by prewarmed culture medium and cells were placed for various time points in a 37°C incubator. After indicated time points, coverslips were transferred to 4% paraformaldehyde, 4% sucrose in PBS, fixed for 20 min, and processed for standard immunofluorescence (Wacker et al., 1997) using Alexa®488- or Alexa®594-coupled secondary anti-rabbit antibodies (Molecular Probes). Endocytosis of βAPP or BACE was normally fully completed after 10–20 min, depending on the individual experiment. Experiments were performed at least twice, and 50–100 cells were scored per cell line and time point. Representative images are shown.

Microscopy

Fixed cells were analyzed on a Leica DMRB microscope equipped with a 100x/1.3 objective and standard FITC and TRITC fluorescence filter sets. Images were obtained using a Spot Camera (RT Monochrome Diagnostics) and the MetaView Imaging software (Universal Imaging Corp.). For analysis of living cells, cells were cultured on poly-L-lysine–coated coverslips and mounted on custom-made aluminum holders. For labeling of the PM, cells were incubated for 20 min on ice in 20 μg/ml TRITC–WGA/PCM (Sigma-Aldrich) followed by a wash in ice cold PBS. Imaging was performed on an Olympus IX70 microscope using a 60 × 1.4 Planapo objective and a GFP/Texas red double dicroic emission filter. Images were recorded with a TILL Vision setup consisting of a TILL Imago camera, Polychrome IV monochromator, and Vision software (T.I.L.L. Photonics GmbH). The EGFP fluorescence in general was very low; typical exposure times ranged from 1–4 s. In cells labeled with TRITC–WGA, special care was taken to avoid excitation of TRICT–WGA when viewing GFP. Excitation with 480–490 nm led to considerable excitation of TRITC–WGA, leading to a bleedthrough of the red fluorescence (due to the double dicroic filter used). Control experiments revealed that excitation with 470 nm showed only GFP, but no TRITC fluorescence, even in very long exposures. Images therefore were recorded with an excitation of 470 nm for GFP and 570 nm for TRITC–WGA.

TIRM

PE or PEASP cells were grown in poly-L-lysine–coated glass bottom dishes (MatTek Corporation). TIRM was performed on an objective type setup based on an inverted microscope (Olympus IX70) equipped with an oil immersion objective (PlanApo ×60, NA 1.45 TIRFM; Olympus). The specimen was illuminated with an argon laser (model 163-All; Spectra Physics). Images were recorded on an Imago CCD sVGA camera using Vision software.

Online supplemental material

The supplemental figures for this article are available at http://www.jcb.org/cgi/content/full/jcb.200201123/DC1. To exclude the possibility that the detection of PS–EGFP at the cell surface is not an artifact of overexpression, we analyzed the subcellular distribution of an overexpressed ER-resident protein. For this, a GFP–ER with a KDEL retention motif was expressed in HEK293 cells and analyzed by conventional fluorescence microscopy (Fig. S1) and TIRM (Fig. S2). No staining of the plasma membrane could be detected.

References

Annaert, W.G., L. Levesque, K. Craessaerts, I. Dierinck, G. Snellings, D. Westaway, P.S. George-Hyslop, B. Cordell, P. Fraser, and B. De Strooper. 1999. Presenilin 1 controls γ-secretase processing of amyloid precursor protein in pre-Golgi compartments of hippocampal neurons. *J. Cell Biol.* 147:277–294.

Bonifacino, J.S., M. Dasso, J. Lippincott-Schwartz, J.B. Harford, and K.M. Yamada. 2000. Current protocols in cell biology. *In* Current Protocols. K. Morgan, editor. John Wiley & Sons Inc., New York. 135–136.

Capell, A., J. Grunberg, B. Pesold, A. Diehlmann, M. Citron, R. Nixon, K. Beyreuther, D.J. Selkoe, and C. Haass. 1998. The proteolytic fragments of the Alzheimer's disease-associated presenilin-1 form heterodimers and occur as a 100-150-kDa molecular mass complex. *J. Biol. Chem.* 273:3205–3211.

Capell, A., H. Steiner, H. Romig, S. Keck, M. Baader, M.G. Grim, R. Baumeister, and C. Haass. 2000a. Presenilin-1 differentially facilitates endoproteolysis of the β-amyloid precursor protein and Notch. *Nat. Cell Biol.* 2:205–211.

Capell, A., H. Steiner, M. Willem, H. Kaiser, C. Meyer, J. Walter, S. Lammich, G. Multhaup, and C. Haass. 2000b. Maturation and pro-peptide cleavage of β-secretase (BACE). *J. Biol Chem.* 275:30849–30854.

Checler, F. 2001. The multiple paradoxes of presenilins. *J. Neurochem.* 76:1621–1627.

Chung, H.M., and G. Struhl. 2001. Nicastrin is required for presenilin-mediated transmembrane cleavage in *Drosophila. Nat. Cell Biol.* 3:1129–1132.

Citron, M., T. Oltersdorf, C. Haass, L. McConlogue, A.Y. Hung, P. Seubert, C. Vigo-Pelfrey, I. Lieberburg, and D.J. Selkoe. 1992. Mutation of the β-amyloid precursor protein in familial Alzheimer's disease increases β-protein production. *Nature.* 360:672–674.

Cupers, P., M. Bentahir, K. Craessaerts, I. Orlans, H. Vanderstichele, P. Saftig, B. De Strooper, and W. Annaert. 2001. The discrepancy between presenilin subcellular localization and γ-secretase processing of amyloid precursor protein. *J. Cell Biol.* 154:731–740.

De Strooper, B., M. Beullens, B. Contreras, L. Levesque, K. Craessaerts, B. Cordell, D. Moechars, M. Bollen, P. Fraser, P.S. George-Hyslop, and F. Van Leuven. 1997. Phosphorylation, subcellular localization, and membrane orientation of the Alzheimer's disease-associated presenilins. *J. Biol. Chem.* 272:3590–3598.

De Strooper, B., P. Saftig, K. Craessaerts, H. Vanderstichele, G. Guhde, W. Annaert, K. Von Figura, and F. Van Leuven. 1998. Deficiency of presenilin-1 inhibits the normal cleavage of amyloid precursor protein. *Nature.* 391:387–390.

De Strooper, B., W. Annaert, P. Cupers, P. Saftig, K. Craessaerts, J.S. Mumm, E.H. Schroeter, V. Schrijvers, M.S. Wolfe, W.J. Ray, et al. 1999. A presenilin-1-dependent γ-secretase-like protease mediates release of Notch intracellular domain. *Nature.* 398:518–522.

Dovey, H.F., V. John, J.P. Anderson, L.Z. Chen, P. de Saint Andrieu, L.Y. Fang, S.B. Freedman, B. Folmer, E. Goldbach, E.J. Holsztynska, et al. 2001. Functional γ-secretase inhibitors reduce β-amyloid peptide levels in brain. *J. Neurochem.* 76:173–181.

Edbauer, D., E. Winkler, C. Haass, and H. Steiner. 2002. Presenilin and nicastrin regulate each other and determine amyloid beta-peptide production via complex formation. *Proc. Natl. Acad. Sci. USA.* 99:8666–8671.

Efthimiopoulos, S., E. Floor, A. Georgakopoulos, J. Shioi, W. Cui, S. Yasothornsrikul, V.Y. Hook, T. Wisniewski, L. Buee, and N.K. Robakis. 1998. Enrichment of presenilin 1 peptides in neuronal large dense-core and somatodendritic clathrin-coated vesicles. *J. Neurochem.* 71:2365–2372.

Esler, W.P., and M.S. Wolfe. 2001. A portrait of Alzheimer secretases–new features and familiar faces. *Science.* 293:1449–1454.

Geling, A., H. Steiner, M. Willem, L. Bally-Cuif, and C. Haass. 2002. A γ-secretase inhibitor blocks Notch signaling in vivo and causes a severe neurogenic phenotype in zebrafish. *EMBO Rep.* 3:688–694.

Georgakopoulos, A., P. Marambaud, S. Efthimiopoulos, J. Shioi, W. Cui, H.C. Li, M. Schutte, R. Gordon, G.R. Holstein, G. Martinelli, et al. 1999. Presenilin-1 forms complexes with the cadherin/catenin cell-cell adhesion system and is recruited to intercellular and synaptic contacts. *Mol. Cell.* 4:893–902.

Goutte, C., M. Tsunozaki, V.A. Hale, and J.R. Priess. 2002. APH-1 is a multipass membrane protein essential for the Notch signaling pathway in *Caenorhabditis elegans* embryos. *Proc. Natl. Acad. Sci. USA.* 99:775–779.

Haass, C., A.Y. Hung, M.G. Schlossmacher, D.B. Teplow, and D.J. Selkoe. 1993. β-Amyloid peptide and a 3-kDa fragment are derived by distinct cellular mechanisms. *J. Biol. Chem.* 268:3021–3024.

Herreman, A., L. Serneels, W. Annaert, D. Collen, L. Schoonjans, and B. De

Strooper. 2000. Total inactivation of γ-secretase activity in presenilin-deficient embryonic stem cells. *Nat. Cell Biol.* 2:461–462.

Hu, Y., Y. Ye, and M.E. Fortini. 2002. Nicastrin is required for gamma-secretase cleavage of the *Drosophila* Notch receptor. *Dev. Cell.* 2:69–78.

Huse, J.T., D.S. Pijak, G.J. Leslie, V.M. Lee, and R.W. Doms. 2000. Maturation and endosomal targeting of beta-site amyloid precursor protein-cleaving enzyme. The Alzheimer's disease beta-secretase. *J. Biol. Chem.* 275:33729–33737.

Kim, S.H., J.Y. Leem, J.J. Lah, H.H. Slunt, A.I. Levey, G. Thinakaran, and S.S. Sisodia. 2001. Multiple effects of aspartate mutant presenilin 1 on the processing and trafficking of amyloid precursor protein. *J. Biol. Chem.* 276:43343–43350.

Kimberly, W.T., W. Xia, T. Rahmati, M.S. Wolfe, and D.J. Selkoe. 2000. The transmembrane aspartates in presenilin 1 and 2 are obligatory for γ-secretase activity and amyloid β-protein generation. *J. Biol. Chem.* 275:3173–3178.

Lah, J.J., and A.I. Levey. 2000. Endogenous presenilin-1 targets to endocytic rather than biosynthetic compartments. *Mol. Cell. Neurosci.* 16:111–126.

Leem, J.Y., S. Vijayan, P. Han, D. Cai, M. Machura, K.O. Lopes, M.L. Veselits, H. Xu, and G. Thinakaran. 2002. Presenilin 1 is required for maturation and cell surface accumulation of nicastrin. *J. Biol. Chem.* 277:19236–19240.

Levitan, D., G. Yu, P. St George Hyslop, and C. Goutte. 2001. APH-2/nicastrin functions in LIN-12/Notch signaling in the *Caenorhabditis elegans* somatic gonad. *Dev. Biol.* 240:654–661.

Li, Y.-M., M.-T. Lai, M. Xu, Q. Huang, J. DiMuzio-Mower, M.K. Sardana, X.-P. Shi, K.-C. Yin, J.A. Shafer, and S.J. Gardell. 2000a. Presenilin 1 is linked with γ-secretase activity in the detergent solubilized state. *Proc. Natl. Acad. Sci. USA.* 97:6138–6143.

Li, Y.-M., M. Xu, M.-T. Lai, Q. Huang, J.L. Castro, J. DiMuzio-Mower, T. Harrison, C. Lellis, A. Nadin, J.G. Neduvelli, et al. 2000b. Photoactivated γ-secretase inhibitors directed to the active site covalently label presenilin 1. *Nature.* 405:689–694.

Lopez-Schier, H., and D.S. Johnston. 2002. *Drosophila* nicastrin is essential for the intramembranous cleavage of notch. *Dev. Cell.* 2:79–89.

Marambaud, P., J. Shioi, G. Serban, A. Georgakopoulos, S. Sarner, V. Nagy, L. Baki, P. Wen, S. Efthimiopoulos, Z. Shao, et al. 2002. A presenilin-1/gamma-secretase cleavage releases the E-cadherin intracellular domain and regulates disassembly of adherens junctions. *EMBO J.* 21:1948–1956.

May, P., Y.K. Reddy, and J. Herz. 2002. Proteolytic processing of LRP mediates regulated release of its intracellular domain. *J. Biol. Chem.* 277:18736–18743.

Möhlmann, T., E. Winkler, X. Xia, D. Edbauer, J. Murell, A. Capell, C. Kaether, H. Zheng, B. Ghetti, C. Haass, and H. Steiner. 2002. Presenilin-1 mutations of leucine 166 equally affect the generation of the Notch and APP intracellular domains independent of their effect on Aβ42 production. *Proc. Natl. Acad. Sci. USA.* 99:8025–8030.

Ni, C.-Y., M.P. Murphy, T.E. Golde, and G. Carpenter. 2001. γ-Secretase cleavage and nuclear localization of ErbB-4 receptor tyrosine kinase. *Science.* 294:2179–2181.

Perez, R.G., S. Soriano, J.D. Hayes, B. Ostaszewski, W. Xia, D.J. Selkoe, X. Chen, G.B. Stokin, and E.H. Koo. 1999. Mutagenesis identifies new signals for beta-amyloid precursor protein endocytosis, turnover, and the generation of secreted fragments, including Abeta42. *J. Biol. Chem.* 274:18851–18856.

Ratovitski, T., H.H. Slunt, G. Thinakaran, D.L. Price, S.S. Sisodia, and D.R. Borchelt. 1997. Endoproteolytic processing and stabilization of wild-type and mutant presenilin. *J. Biol. Chem.* 272:24536–24541.

Ray, W.J., M. Yao, J. Mumm, E.H. Schroeter, P. Saftig, M. Wolfe, D.J. Selkoe, R. Kopan, and A.M. Goate. 1999. Cell surface presenilin-1 participates in the γ-secretase-like proteolysis of Notch. *J. Biol. Chem.* 274:36801–36807.

Sastre, M., H. Steiner, K. Fuchs, A. Capell, G. Multhaup, M.M. Condron, D.B. Teplow, and C. Haass. 2001. Presenilin-dependent gamma-secretase processing of β-amyloid precursor protein at a site corresponding to the S3 cleavage of Notch. *EMBO Rep.* 2:835–841.

Saura, C.A., T. Tomita, S. Soriano, M. Takahashi, J.Y. Leem, T. Honda, E.H. Koo, T. Iwatsubo, and G. Thinakaran. 2000. The nonconserved hydrophilic loop domain of presenilin (PS) is not required for PS endoproteolysis or enhanced abeta 42 production mediated by familial early onset Alzheimer's disease-linked PS variants. *J. Biol. Chem.* 275:17136–17142.

Saxena, M.T., E.H. Schroeter, J.S. Mumm, and R. Kopan. 2001. Murine notch homologs (n1-4) undergo presenilin-dependent proteolysis. *J. Biol. Chem.* 276:40268–40273.

Schroeter, E.H., J.A. Kisslinger, and R. Kopan. 1998. Notch-1 signalling requires ligand-induced proteolytic release of intracellular domain. *Nature.* 393:382–386.

Schwarzman, A.L., N. Singh, M. Tsiper, L. Gregori, A. Dranovsky, M.P. Vitek, C.G. Glabe, P.H. St George-Hyslop, and D. Goldgaber. 1999. Endogenous

presenilin 1 redistributes to the surface of lamellipodia upon adhesion of Jurkat cells to a collagen matrix. *Proc. Natl. Acad. Sci. USA.* 96:7932–7937.

Selkoe, D.J. 1999. Translating cell biology into therapeutic advances in Alzheimer's disease. *Nature.* 399:A23–A31.

Singh, N., Y. Talalayeva, M. Tsiper, V. Romanov, A. Dranovsky, D. Colflesh, G. Rudamen, M.P. Vitek, J. Shen, X. Yang, et al. 2001. The role of Alzheimer's disease-related presenilin 1 in intercellular adhesion. *Exp. Cell Res.* 263:1–13.

Steiner, H., K. Duff, A. Capell, H. Romig, M.G. Grim, S. Lincoln, J. Hardy, X. Yu, M. Picciano, K. Fechteler, et al. 1999a. A loss of function mutation of presenilin-2 interferes with amyloid β-peptide production and Notch signaling. *J. Biol. Chem.* 274:28669–28673.

Steiner, H., H. Romig, M.G. Grim, U. Philipp, B. Pesold, M. Citron, R. Baumeister, and C. Haass. 1999b. The biological and pathological function of the presenilin-1 Δexon 9 mutation is independent of its defect to undergo proteolytic processing. *J. Biol. Chem.* 274:7615–7618.

Steiner, H., H. Romig, B. Pesold, U. Philipp, M. Baader, M. Citron, H. Loetscher, H. Jacobsen, and C. Haass. 1999c. Amyloidogenic function of the Alzheimer's disease-associated presenilin 1 in the absence of endoproteolysis. *Biochemistry.* 38:14600–14605.

Steiner, H., M. Kostka, H. Romig, G. Basset, B. Pesold, J. Hardy, A. Capell, L. Meyn, M.G. Grim, R. Baumeister, et al. 2000. Glycine 384 is required for presenilin-1 function and is conserved in polytopic bacterial aspartyl proteases. *Nat. Cell Biol.* 2:848–851.

Takashima, A., M. Sato, M. Mercken, S. Tanaka, S. Kondo, T. Honda, K. Sato, M. Murayama, K. Noguchi, Y. Nakazato, and H. Takahashi. 1996. Localization of Alzheimer-associated presenilin 1 in transfected COS-7 cells. *Biochem. Biophys. Res. Commun.* 227:423–426.

Thinakaran, G., D.R. Borchelt, M.K. Lee, H.H. Slunt, L. Spitzer, G. Kim, T. Ratovitsky, F. Davenport, C. Nordstedt, M. Seeger, et al. 1996. Endoproteolysis of presenilin 1 and accumulation of processed derivatives in vivo. *Neuron.* 17:181–190.

Thinakaran, G., C.L. Harris, T. Ratovitski, F. Davenport, H.H. Slunt, D.L. Price, D.R. Borchelt, and S.S. Sisodia. 1997. Evidence that levels of presenilins (PS1 and PS2) are coordinately regulated by competition for limiting cellular factors. *J. Biol. Chem.* 272:28415–28422.

Toomre, D., and D.J. Manstein. 2001. Lighting up the cell surface with evanescent wave microscopy. *Trends Cell Biol.* 11:298–303.

Vassar, R., and M. Citron. 2000. Aβ-generating enzymes: recent advances in β- and γ-secretase research. *Neuron.* 27:419–422.

Wacker, I., C. Kaether, A. Kromer, A. Migala, W. Almers, and H.H. Gerdes. 1997. Microtubule-dependent transport of secretory vesicles visualized in real time with a GFP-tagged secretory protein. *J. Cell Sci.* 110:1453–1463.

Walter, J., A. Capell, J. Grunberg, B. Pesold, A. Schindzielorz, R. Prior, M.B. Podlisny, P. Fraser, P.S. Hyslop, D.J. Selkoe, and C. Haass. 1996. The Alzheimer's disease-associated presenilins are differentially phosphorylated proteins located predominantly within the endoplasmic reticulum. *Mol. Med.* 2:673–691.

Walter, J., R. Fluhrer, B. Hartung, M. Willem, C. Kaether, A. Capell, S. Lammich, G. Multhaup, and C. Haass. 2001. Phosphorylation regulates intracellular trafficking of beta-secretase. *J. Biol. Chem.* 276:14634–14641.

Wiltfang, J., A. Smirnov, B. Schnierstein, G. Kelemen, U. Matthies, H.W. Klafki, M. Staufenbiel, G. Huther, E. Ruther, and J. Kornhuber. 1997. Improved electrophoretic separation and immunoblotting of β-amyloid (Aβ) peptides 1-40, 1-42, and 1-43. *Electrophoresis.* 18:527–532.

Wolfe, M.S., and C. Haass. 2001. The role of presenilins in γ-secretase activity. *J. Biol. Chem.* 276:5413–5416.

Wolfe, M.S., J. De Los Angeles, D.D. Miller, W. Xia, and D.J. Selkoe. 1999a. Are presenilins intramembrane-cleaving proteases? Implications for the molecular mechanism of Alzheimer's disease. *Biochemistry.* 38:11223–11230.

Wolfe, M.S., W. Xia, B.L. Ostaszewski, T.S. Diehl, W.T. Kimberly, and D.J. Selkoe. 1999b. Two transmembrane aspartates in presenilin-1 required for presenilin endoproteolysis and γ-secretase activity. *Nature.* 398:513–517.

Yamazaki, T., E.H. Koo, and D.J. Selkoe. 1996. Trafficking of cell-surface amyloid beta-protein precursor. II. Endocytosis, recycling and lysosomal targeting detected by immunolocalization. *J. Cell Sci.* 109:999–1008.

Yu, G., M. Nishimura, S. Arawaka, D. Levitan, L. Zhang, A. Tandon, Y.Q. Song, E. Rogaeva, F. Chen, T. Kawarai, et al. 2000. Nicastrin modulates presenilin-mediated notch/glp-1 signal transduction and betaAPP processing. *Nature.* 407:48–54.

Zhang, Z., P. Nadeau, W. Song, D. Donoviel, M. Yuan, A. Bernstein, and B.A. Yankner. 2000. Presenilins are required for γ-secretase cleavage of β-APP and transmembrane cleavage of Notch-1. *Nat. Cell Biol.* 2:463-465.